Catalysis Today 161 (2011) 84–90

Contents lists available at ScienceDirect

Catalysis Today

journal homepage: www.elsevier.com/locate/cattod

Anatase nanoparticles from hydrated titania gels

Petra Pulišová*, Jaroslav Boháček, Jan Šubrt, Lórant Szatmáry, Petr Bezdička, Nataliya Murafa

Institute of Inorganic Chemistry of the AS CR, v.v.i., 250 68 Husinec-Řež, Czech Republic

ARTICLE INFO

Article history:
Received 18 June 2010
Received in revised form 2 December 2010
Accepted 6 December 2010
Available online 11 January 2011

Keywords:
Anatase particles
Annealing
Titania nanopaticles
Photocatalyst

ABSTRACT

The growth of anatase particles during annealing up to 1000 °C of the dried precipitates prepared by neutralization of $TiOSO_4$ aqueous solutions with aqueous ammonia until desired pH value at temperatures 0–80 °C was studied. The crystallinity of the precipitates depends significantly on the precipitation temperature; the precipitates prepared at low temperatures were almost amorphous whereas the higher precipitation temperature leads to more crystalline samples. Heating the sample results in crystallization of the amorphous part and above ~400–500 °C the sample is fully crystalline. Contemporary with the crystallization of the amorphous part significant decrease of the crystal cell volume was observed in the same temperature region. Above this temperature monotonous changes in crystal lattice constants (growth of the *a* and decrease of the *c* parameter) resulting in decrease of the crystal cell size was observed. Growth of anatase nanocrystals and disappearance of surface amorphous layer was observed above 600 °C. All samples were highly photoactive. The fastest 4-chlorophenol decomposition corresponding to highest photocatalytic activity was found at samples annealed at the temperature around 800–850 °C corresponding to the particles ~70 nm in diameter.

1. Introduction

Titania nanoparticles are used as photocatalyst in many applications, laboratory and industrial. Several procedures were suggested to synthesize nano TiO_2 in order to control its properties. For industrial applications of photocatalysis, like photocatalytic paints, concrete, etc. the price of photocatalyst plays a significant role in determining the success of any intended project in this area [1–10]. For these reasons, modification of processes used for anatase pigment manufacture to prepare titania nanoparticles will provide advantages for production of nano TiO_2 in industrial scale.

One of the promising ways to manufacture nanoparticles of TiO_2 is calcination of intermediates originating in the sulphate technology of titania white pigment production. The starting material, formed during hydrolysis of a titanyl sulphate solution, consists of a mixture of amorphous and nanocrystalline titanium oxide particles and is conventionally converted to white titania pigments by controlled calcination in a rotary kiln [11–14] until the pigment size particles (~250 nm) are obtained. During this process growth of anatase particles proceeds, which can be stopped in any stage providing anatase nanocrystals, shape and size of which depends on the annealing conditions. It was demonstrated recently that careful control of the preparation conditions during $TiOSO_4$ hydrolysis and subsequent calcination can be used to fine tuning of the resulting photocatalyst properties, sometimes exceeding the standard Degussa P 25 TiO_2 [15,16]. However, the process of nanoparticles formation is described insufficiently regardless of technical importance of the process.

We studied the growth of anatase particles during annealing up to 1000 °C of the dried precipitates prepared by neutralization of $TiOSO_4$ aqueous solutions with aqueous ammonia until desired pH value at temperatures 0–80 °C. The products were structurally characterized and their photoactivity was determined by measuring the kinetics of photocatalysed decomposition of 4-chlorophenol in water.

2. Methods

2.1. Sample preparation

4.80 g of titanyl sulphate ($TiOSO_4 \cdot xH_2O$) was taken as the precursor and 150 mL of distilled water was added to it and kept in stirring at 35 °C till the solution is color-less. The solution was stirred at approx. 20, 40 and 80 °C and ammonia solution was added drop by drop to precipitate the product. The pH value, temperature of the solution and the volume of ammonia solution added was noted. Ammonia solution was added till the pH of the solution reaches approx. 3, 6 and 8. After precipitation the product was filtered with distilled water and few times washed with isopropanol. Products were dried in air at room temperature.

* Corresponding author.
E-mail address: pulisovap@yahoo.com (P. Pulišová).

0920-5861/$ – see front matter © 2010 Elsevier B.V. All rights reserved.
doi:10.1016/j.cattod.2010.12.032

2.2. Characterization of the samples

The solid samples were characterized using powder X-ray diffraction analysis, thermogravimetry, differential thermal analysis, mass spectrometry, transmission electron microscopy and scanning electron microscopy coupled with EDS analyzer, the surface area was determined by the BET method.

The X-ray diffractions diagrams were recorded with a PHILPS X'pert Pro equipped with the X'celerator. Cu K_α radiation and a nickel filter were used. A voltage of 40 kV and an intensity of 40 mA were employed. The percentages of anatase, rutile and the high pressure Titania phase (TiO_2II) with structure α-PbO_2 were determined by the direct method from the intensity of the diffraction peaks (1 1 0) of rutile (1 0 1) of anatase and (1 1 1) [17]. The crystal sizes were determined from the integral broadening of the diffraction peaks corresponding to the planes (1 0 1) of anatase (1 1 0) of rutile, respectively. The percentages of individual components were determined from the intensities of the reflections by the direct method of Cullity and Stock [17]. The content of amorphous component was determined by Standard addition method using pure crystalline ZnO as standard.

Transmission electron micrographs were obtained using a JEOL JEM 3010 microscope operating at accelerating voltage of 300 kV. The samples for electron microscopy were prepared using grinding and dispersing the powder in propyl alcohol and applying a drop of very dilute suspension on carbon coated grids. The suspensions were dried by slow evaporation at ambient temperature.

Structural morphology of the samples was revealed by SEM (Scanning Electron Microscopy). A Philips XL 30 CP microscope equipped with EDX (Energy Dispersive X-ray), Robinson, SE (Secondary Electron) and BSE (Back-Scattered Electron detectors) was used. For the observations in SE electrons the samples were coated with thin conductive Au–10%Pd alloy layer. The EDX information is correct to about ±3%.

The thermogravimetry (TG) and differential thermal analysis (DTA) and mass spectrometry (MS) measurements were carried out heating in air by using the equipment NETZSCH STA 409 MS. The dried fine powders of synthesized samples TiO_2 were used for measurements. The heating rate was 10 °C min^{-1} (from 20 to 1200 °C).

Specific surface area was determined by the BET (Brunauer–Emmett–Teller) [18] method form nitrogen adsorption–desorption isotherm acquired at liquid-nitrogen temperature using a NOVA 4200e instrument with a 15-min outgas at 120 °C.

Kinetics of decay of 0.14 mmol L^{-1} solution of 4-chlorophenol (4-CP) in 70 mL of aerated aqueous suspension of mixtures with the tested photocatalysts (1 g L^{-1}) were monitored. The laboratory irradiation experiments were performed in a self-constructed photo reactor at temperature 20 °C. It consists of two coaxial quartz tubes placed in the middle of a steel cylinder with an aluminum foil

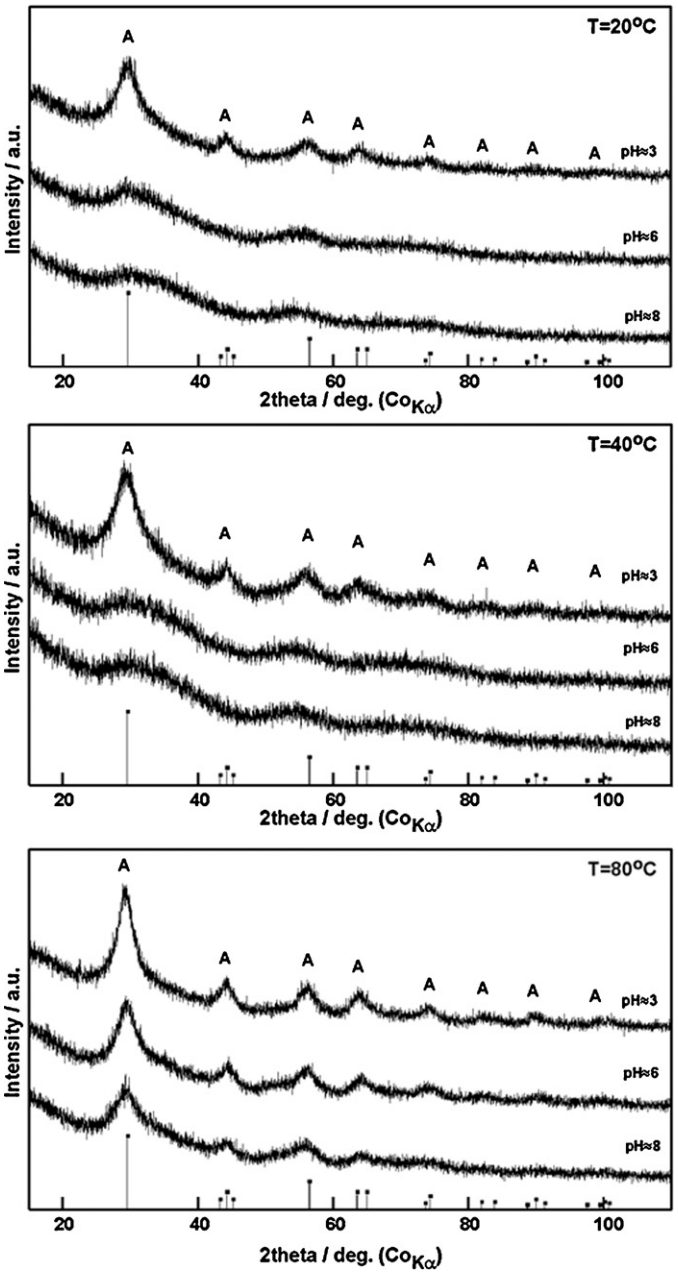

Fig. 1. XRD of the dried precipitates prepared at different pH and temperatures.

Table 1
Summary of the conditions of the prepared samples and their properties.

Sample	Preparation conditions		Structural parameters			Sample properties	
	Temperature	pH	Cell volume [Å^3]	*a* [Å]	*c* [Å]	Sulphur content [wt.%]	Surface area [m^2/g]
TIG 10	20 °C	3	137.31	3.7978	9.5199	4.41	100
TIG 11	20 °C	6	140.39	3.8161	9.6405	0.11	205
TIG 12	20 °C	8	–	–	–	0.08	215
TIG 13	40 °C	3	137.47	3.7987	9.5266	2.90	70
TIG 14	40 °C	6	–	–	–	0.11	248
TIG 15	40 °C	8	–	–	–	0.15	256
TIG 16	80 °C	3	136.96	3.7957	9.5061	3.22	91
TIG 17	80 °C	6	136.91	3.8017	9.4727	0.05	186
TIG 18	80 °C	8	137.00	3.8060	9.4575	0.17	223

covering its inner wall. Inner quartz tube (diameter 24 mm, length 300 mm) was filled with the investigated suspension (70 mL) and magnetically stirred. Cooling water was circulated between the inner and the outer quartz tube to keep constant temperature of 20 °C. The detailed description of the photo reactor is given in [19]. The light sources were placed close to the quartz tubes. By means of the ferric oxalate actinometry, an average light intensity entering the volume of 50–70 mL of the irradiated solution was determined as $I_0 = 5.3 \times 10^{-5}$ Einstein dm^{-3} s^{-1}. The TiO_2 mixtures were sonicated for 20 min with a sonicator (230 W, 30 kHz) before use. The pH of the resulting suspension was taken as the initial value for neutral conditions and under the experiment was kept at pH 7.00 was measured using an Alpha 500 pH meter equipped with a glass pH electrode. Probes of irradiated suspensions (1 mL) were taken at appropriate irradiation times. The solid photocatalyst (necessarily together with the adsorbed portions of the dissolved molecular species) was removed before HPLC, employing filtration by a Millipore syringe adapter (diameter 13 mm) with filter 408 (porosity 0.45 μm). The HPLC experiments were run on a Merck device with L-6200 Intelligent Pump, L-3000 Photo Diode Array Detector and D-2500 Chromato-Integrator. Mobile phase methanol/water (2:3, v/v) and a Merck column LiChro-CART 125-4 filled with LiChrosphere 100 RP-18 (5 mm) were used, injection loop was 20 mL, flow rate 1 mL min^{-1} and detection wavelength 280 nm were applied.

3. Results and discussion

Fig. 1 shows the XRD patterns of dried precipitates prepared at various temperatures and pH values. Properties of the precipitates are summarised in Table 1. The XRD diffraction pattern is typical for nanocrystalline anatase. We can see that the crystallinity of the precipitates depends significantly on the precipitation temperature; the precipitates prepared at low temperatures were almost amorphous whereas the higher precipitation temperature leads to more crystalline samples. We observed that even the relatively well crystalline samples prepared at 80 °C contain indispensable amount of X-ray amorphous component reaching approx. 30% by weight.

With increasing pH value from 3 to 6, grain boundaries start forming between the anatase particles and also the amount of sulphur is reduced (see Table 1). Influence of these processes result in reducing the volume of the anatase particles and the specific surface area. By further increasing the pH value up to 8, the particle size decreases and the specific surface area was found to be increasing. From X-ray diffractograms (Fig. 1) we can see that sample TIG 16 prepared at temperature 80 °C contains the most crystalline anatase particles in comparison with samples prepared at lower temperatures. In comparison of the diffractograms of samples prepared at various pH values we can see that with increasing pH values samples were practically amorphous.

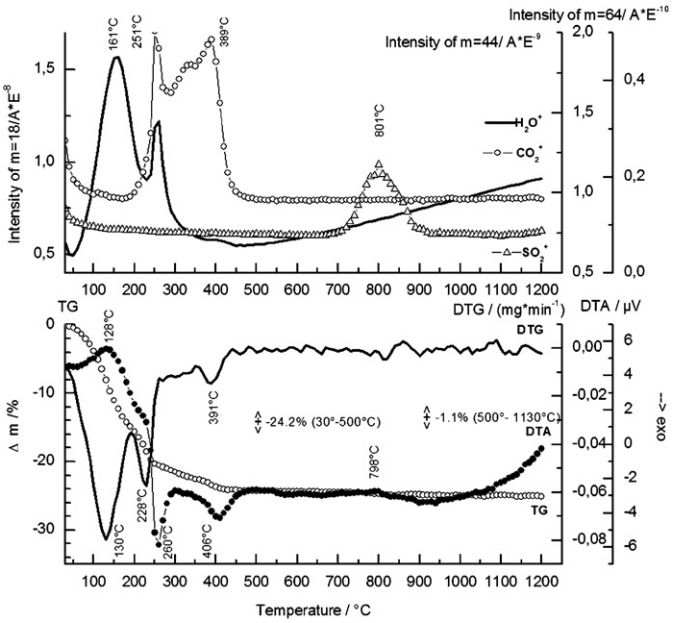

Fig. 2. DTG, TG, DTA and EG (MS) results of the sample TIG 11 measured in air.

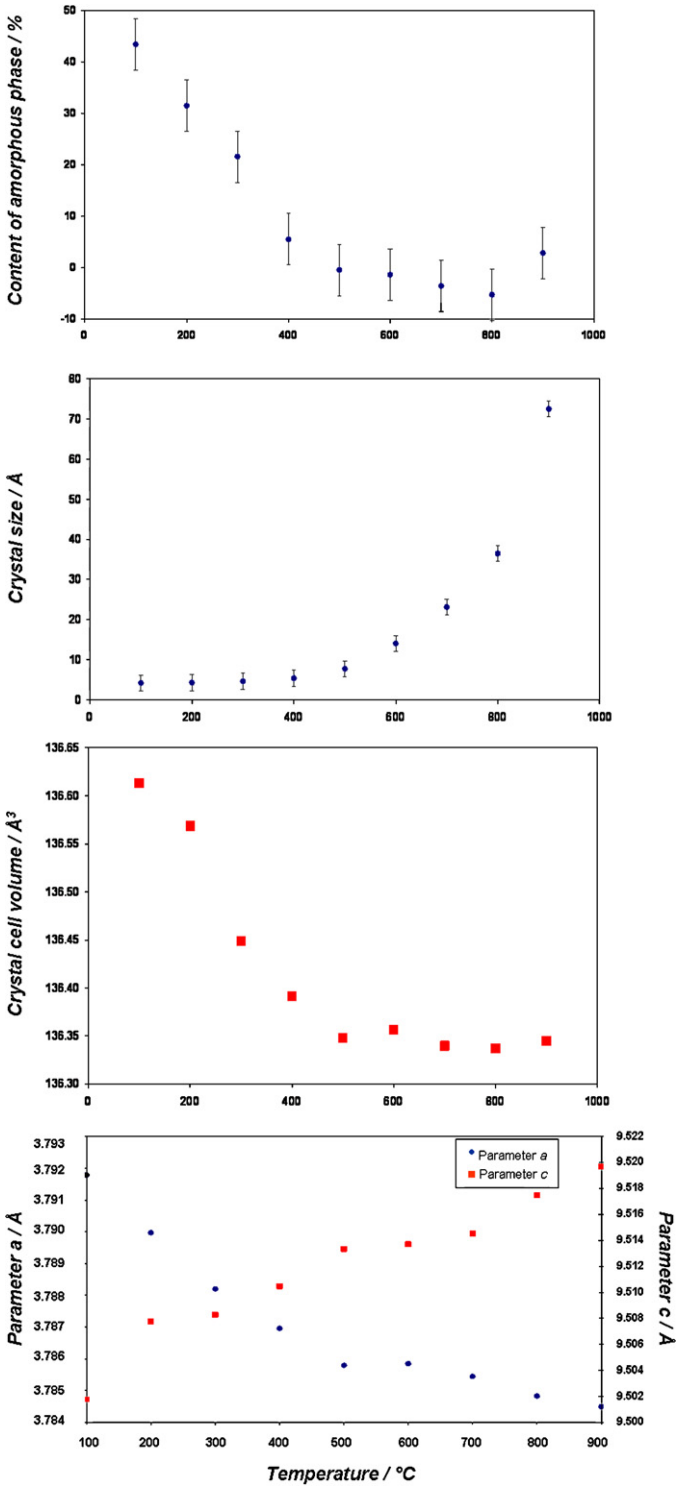

Fig. 3. Changes of structural parameters of the sample TIG 16 with annealing temperature.

Results of thermal analysis measurements (Differential Thermal Analysis – DTA, Thermogravimetry – TG, DTG and Evolved Gas Analysis – EGA) are given in Fig. 2. We can conclude from this Figure that main amount of adsorbed water is released in temperature range 100–300 °C indicting stronger binding of this component than pure physical adsorption. The sample contains also small amount of CO_2, probably result of adsorption of this gas from air due to high surface area of the sample. This component is released between 200 and 500 °C; this fact indicates also relatively strong bond of CO_2 in the precipitate structure. The sample contains also small amount of sulphates, resulting SO_2 is released between 700 and 900 °C. These results indicate that whereas the starting sample is rather complicated mixture of few components, above ~700 °C the sample is practically pure crystalline anatase.

Changes of structural parameters of the sample TIG 16 (prepared at 80 °C, pH 3) with annealing temperature are given in Fig. 3. Whereas the freshly precipitated sample contains, except of anatase nanocrystals, also significant part of amorphous component, heating the sample results in crystallization of the amorphous part and above ~400–500 °C the sample is fully crystalline. Contemporary with the crystallization of the amorphous part we observe in the same temperature region also significant decrease of the crystal cell volume (see Fig. 3). That means that highly defect crystal lattice which forms the freshly precipitated sample is ordered and the defects present are eliminated on heating at ~500 °C and above. Above this temperature up to ~600 °C we observed monotonous changes in crystal lattice constants (growth of the *a* and decrease of the *c* parameter) resulting in decrease of the crystal cell size (see Fig. 3). All these phenomena are associated with elimination of the lattice defects present in the fresh precipitated sample. Release of some impurities like H_2O, SO_2 and CO_2 which are present in the starting material in small but not negligible amounts accompanies these changes. Although we have not any direct evidence concerning the nature of the defects eliminated, very similar phenomenon was observed on α-Fe_2O_3 (hematite) precipitated from the aqueous media by Wolska [20,21]. She proposed that part of the O^{2-} anions in the structure of precipitated hematite is replaced by OH^- and the charge compensation is achieved by formation of vacancies on the Fe^{3+} positions. This model explains presence of structurally bound H_2O in this form of hematite, which is fully released only at relatively high temperatures. Similar model is acceptable also for TiO_2 prepared from an aqueous media and can explain behaviour of this material on heating.

The changes of anatase crystallite size with increasing heating temperature for sample prepared at 80 °C are given in Fig. 3. There are no observable changes of crystallite size up to ~500–600 °C, above this temperature sudden growth of crystallites occur reaching almost the pigment size (~100 nm) at 900–1000 °C. Thus, the starting sample is formed by randomly oriented 4–6 nm anatase crystals embedded in amorphous material (see also Figs. 4–6). After annealing to 800 °C, small regular anatase single crystal ~70 nm were formed (see Fig. 6).

The conclusions based on the analysis of the XRD patterns are in good agreement with observations obtained by electron microscopy (HRTEM). Micrographs of the initial sample prepared at 80 °C and pH 3 are given in Fig. 4. In Fig. 4A and B we

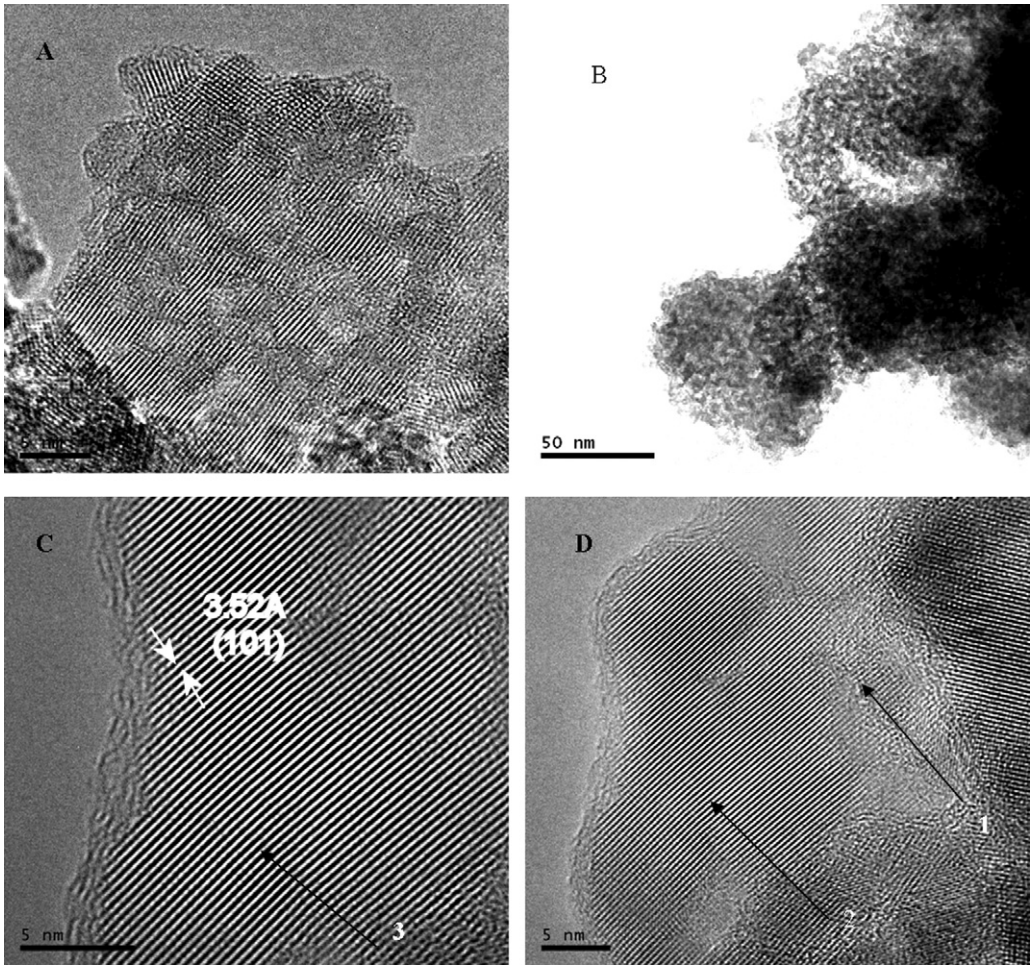

Fig. 4. HRTEM micrographs of the initial sample TIG 16. The arrows in micrographs C and D indicate the grain boundaries between the original nanograins of TiO_2.

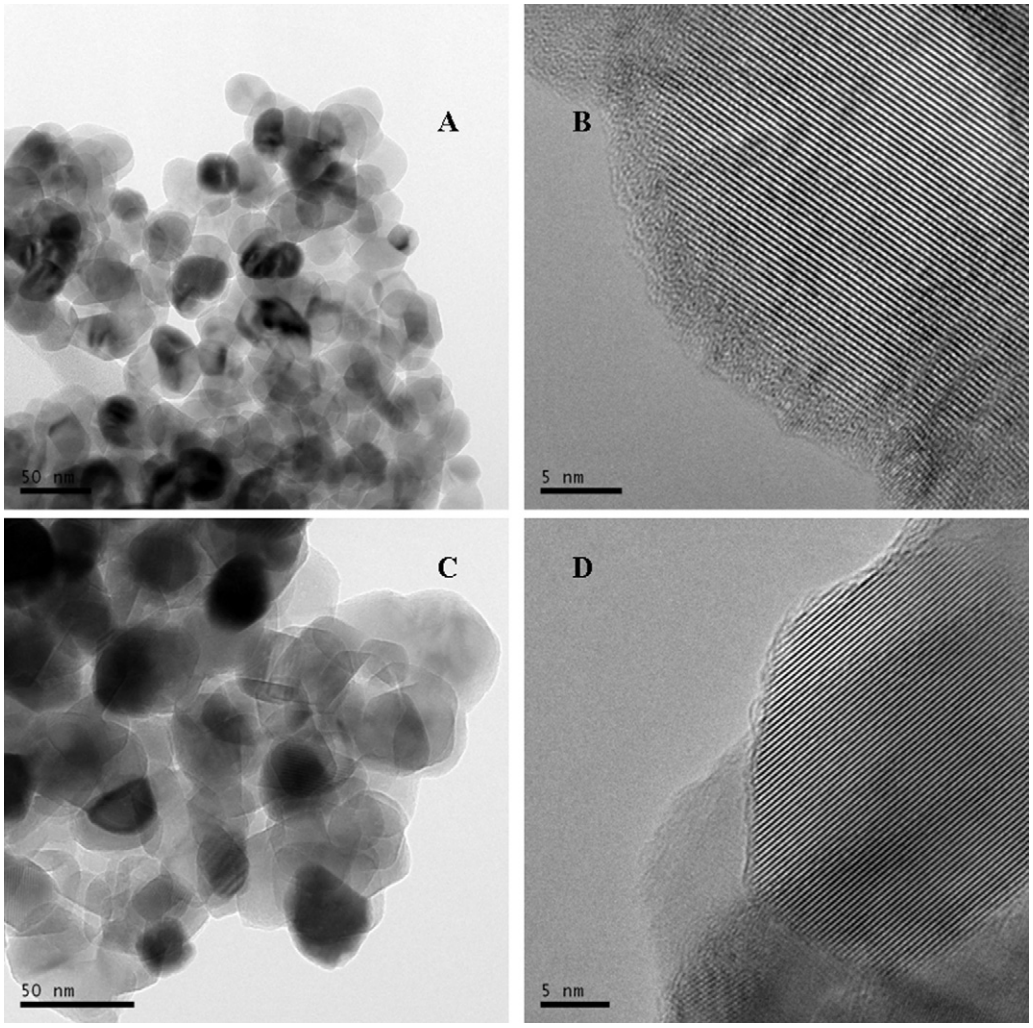

Fig. 5. HRTEM micrographs of the sample TIG 16 annealed at 700 °C. Micrographs A and B – annealing time 30 min; Micrographs C and D – annealing time 8 h.

observe nanocrystals of anatase 2–5 nm in size embedded in an amorphous material. Continuing crystallization was observed in different points of the same sample (see Fig. 4C and D). We observe small grains of size ~5 nm mutually intergrown, but the grain boundaries are still visible. The crystal lattice reaches much bigger volume than the original crystals but the fringes are slightly tilted in the points of contact of the original grains (see arrows 2 and 3 in Fig. 4C and D). Such observations agree well with the concept of oriented crystal growth originally proposed by Buyanov [22] and recently confirmed on the basis of HRTEM observations by Banfield for crystallization of $Fe(OH)_3$ in aqueous media. Authors expect that adjacent 2- to 3-nanometer particles aggregate and rotate so their structures adopt parallel orientations in three dimensions. Crystal growth is accomplished by eliminating water molecules at interfaces and forming iron–oxygen bonds. Self-assembly occurs at multiple sites, leading to a coarser, polycrystalline material. Point defects (from surface-adsorbed impurities), dislocations, and slabs of structurally distinct material are created as a consequence of this growth mechanism and can dramatically impact subsequent reactivity. This mechanism described for growth of α-Fe_2O_3 nanocrystals can be successfully extended to TiO_2 crystallization and can help to explain the peculiar properties of TiO_2 crystals originated from an aqueous media and heated to low temperatures in water.

HRTEM micrographs of the initial sample prepared at 80 °C and pH 3 annealed at 700 °C and 800 °C for different time (30 min and 8 h) are given in Figs. 5 and 6, respectively. The sample annealed at 700 °C for 30 min (Fig. 5A and B) shows crystalline anatase nanoparticles on the surface of which 2–3 nm thick amorphous layer is clearly visible. Prolonged annealing at the same temperature for 8 h led to increase of particle size and significant thinning of the amorphous surface layer. At 800 °C the view is similar, particles are significantly bigger at after annealing for 8 h the amorphous surface layer disappeared almost completely.

All fresh precipitated samples are highly photoactive. Results of measurement of kinetics of decomposition of 4-chlorophenol are given in Figs. 7–9. Experimental dependences of the molar concentrations of 4-chlorophenol on the irradiation time were fitted by nonlinear regression employing first order kinetics. As a result, optimized values of the initial concentrations of 4-chlorophenol and the first order rate constants were obtained. In Fig. 9, these rate constants are shown as a function of annealing temperature for the particular photocatalyst samples. We can see fast decrease in 4-chlorophenol concentration with the time of irradiation, comparable and for some samples even faster than the Degussa P 25 sample used as standard sample for comparison. We observed that the fastest decomposition (highest photocatalytic activity) was found for samples annealed at the temperature around 800–850 °C corresponding to the particles ~70 nm diameter. At much higher temperatures the photoactivity of the sample decreased owing to too big particles and transformation to rutile. On the contrary, the lowest activity was observed for the starting sample containing the smallest nanoparticles of TiO_2 approx. 4–5 nm. We can conclude

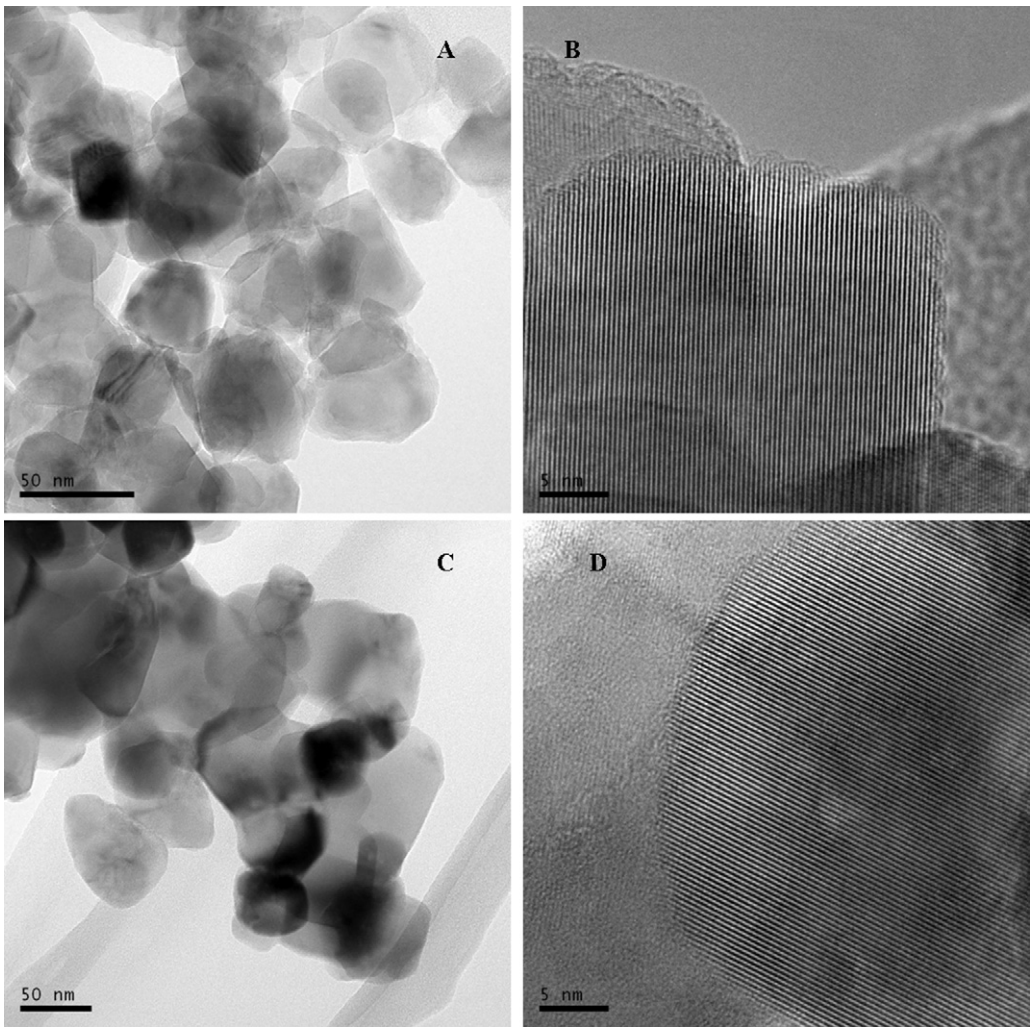

Fig. 6. HRTEM micrographs of the sample TIG 16 annealed at 800 °C. Micrographs A and B – annealing time 30 min; Micrographs C and D – annealing time 8 h.

that annealing of nanocrystalline TiO_2 formed by precipitation of solutions of $TiOSO_4$ can be used for preparation of highly photoactive material by controlled annealing. The process is accompanied by changes of crystallinity and elimination of crystal defects.

During the heat treatment of starting sample TIG 16 the diameter of anatase particles is changing and the shape (spherical) remains same. It is obvious, that with increasing temperature of the heat treatment the diameter of the anatase particles is increasing

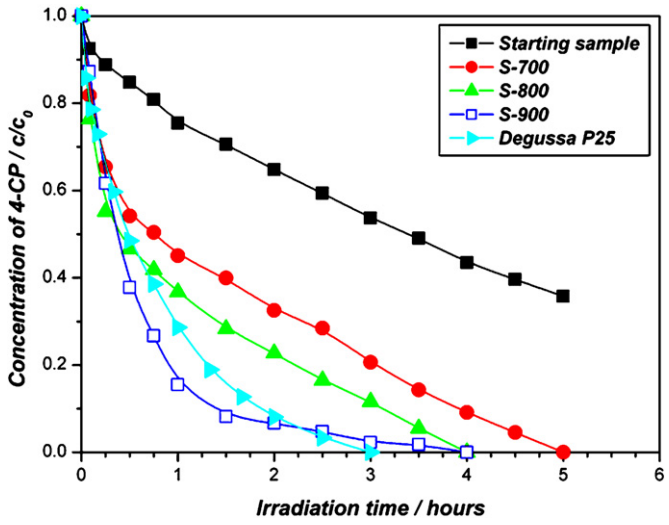

Fig. 7. Photoactivity of TiO_2 samples prepared by annealing of the sample TIG 16 at various temperatures in comparison with the Degussa P 25 photocatalyst.

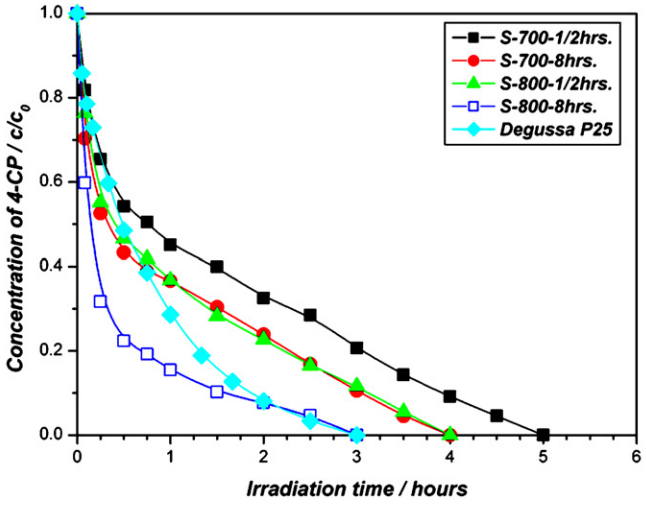

Fig. 8. Photoactivity of TiO_2 samples prepared by annealing of the sample TIG 16 annealed at 700 and 800 °C at 30 min and 8 h in comparison with the Degussa P 25 photocatalyst.

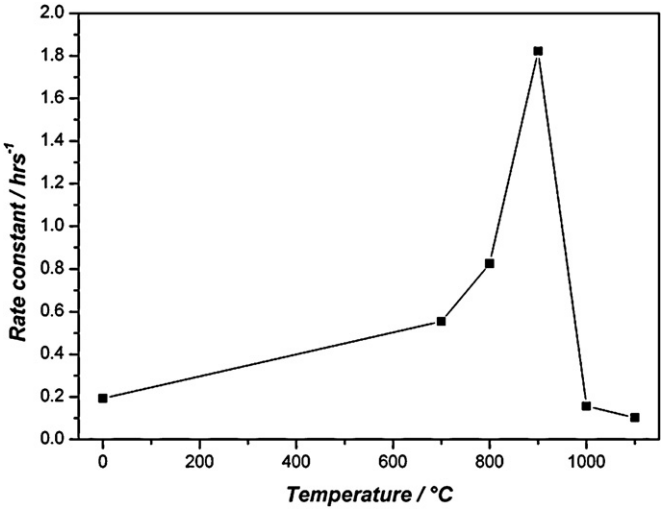

Fig. 9. Dependence of the rate constant of photocatalysed decomposition of 4-chlorophenol on the annealing temperature. Starting sample TIG 16.

(Figs. 4 and 5) which means the surface to volume ratio increases supporting better photocatalytic reactions. This was the reason why the sample heated up to 900 °C was most photoactive. Further increasing of temperature up to 1000 °C (Fig. 9) results in rapid fall down of photoactivity as a consequence of transformation of anatase to rutile.

4. Conclusions

The growth of anatase particles during annealing up to 1000 °C of the dried precipitates prepared by neutralization of $TiOSO_4$ aqueous solutions with aqueous ammonia until desired pH value at temperatures 0–80 °C was studied. The crystallinity of the precipitates depends significantly on the precipitation temperature; the precipitates prepared at low temperatures were almost amorphous whereas the higher precipitation temperature leads to more crystalline samples. Heating the sample results in crystallization of the amorphous part and above ~400–500 °C the sample is fully crystalline. Contemporary with the crystallization of the amorphous part significant decrease of the crystal cell volume was observed in the same temperature region. Above this temperature monotonous changes in crystal lattice constants (growth of the *a* and decrease of the *c* parameter) resulting in decrease of the crystal cell size was observed. Growth of anatase nanocrystals and disappearance of surface amorphous layer was observed above 600 °C. All samples were highly photoactive. The fastest 4-chlorophenol decomposition corresponding to highest photocatalytic activity was found at samples annealed at the temperature around 800–850 °C corresponding to the particles ~70 nm diameter.

Acknowledgment

This work was supported by the Ministry of Education, Youth and Sports of the Czech Republic (project no. lM4531477201).

References

[1] M. Anpo, M. Takeuchi, J. Catal. 216 (2003) 505.
[2] A. Fujishima, X.T. Zhang, D.A. Tryk, Surf. Sci. Rep. 63 (2008) 515.
[3] E. Kociolek-Balawejder, M. Szymczyk, Przem. Chem. 86 (2007) 1179.
[4] A. Kudo, Y. Miseki, Chem. Soc. Rev. 38 (2009) 253.
[5] G. Liu, L.Z. Wang, H.G. Yang, H.M. Cheng, G.Q. Lu, J. Mater. Chem. 20 (2010) 831.
[6] J.F. Luan, K. Ma, L.Y. Zhang, M. Li, Y.M. Li, B.C. Pan, Curr. Org. Chem. 14 (2010) 683.
[7] M. Ni, M.K.H. Leung, D.Y.C. Leung, K. Sumathy, Renew. Sust. Energy Rev. 11 (2007) 401.
[8] N.N. Rao, P. Natarajan, Curr. Sci. 66 (1994) 742.
[9] E. Serrano, G. Rus, J. Garcia-Martinez, Renew. Sust. Energy Rev. 13 (2009) 2373.
[10] R. Strobel, A. Baiker, S.E. Pratsinis, Adv. Powder Technol. 17 (2006) 457.
[11] U. Gesenhues, Chem. Eng. Technol. 24 (2001) 685.
[12] B. Grzmil, D. Grela, B. Kic, in: 35th International Conference of the Slovak-Society-of-Chemical-Engineering, Tatranske Matliare, SLOVAKIA, May 26–30 2008.
[13] B. Grzmil, D. Grela, B. Kic, Pol. J. Chem. Technol. 11 (2009) 15.
[14] B. Grzmil, D. Grela, B. Kic, Chem. Pap. 63 (2009) 217.
[15] S. Sakthivel, M.C. Hidalgo, D.W. Bahnemann, S.U. Geissen, V. Murugesan, A. Vogelpohl, Appl. Catal. B-Environ. 63 (2006) 31.
[16] M.C. Hidalgo, D. Bahnemann, Appl. Catal. B-Environ. 61 (2005) 259.
[17] B.D. Cullity, S.R. Stock, Elements of X-ray Diffraction, Prentice Hall, New York, 2001.
[18] S. Brunauer, P.H. Emmet, E. Teller, J. Am. Chem. Soc. 60 (1938) 309.
[19] S. Bakardjieva, J. Subrt, V. Stengl, M.J. Dianez, M.J. Sayagues, Appl. Catal. B-Environ. 58 (2005) 193.
[20] E. Wolska, Zeitschrift Fur Kristallographie 154 (1981) 69.
[21] E. Wolska, W. Szajda, J. Mater. Sci. 20 (1985) 4407.
[22] R.A. Buyanov, O.P. Krivoruchko, Izv. Sib. Otd. Akad. Nauk SSSR Seriya Khim. Nauk (1982) 28.